

Chapter 14

Value-Added Products from Wastes Using Extremophiles in Biorefineries: Process Modeling, Simulation, and Optimization Tools



Elias Martínez-Hernández, Kok Siew Ng, Myriam A. Amezcua Allieri, Jorge A. Aburto Anell, and Jhuma Sadhukhan

List of Abbreviations

ATP	Adenosine triphosphate
CHP	Combined heat and power
CSTR	Continuously stirred tank reactor
GHG	Greenhouse gas
GWP	Global warming potential
LCA	Life cycle assessment
MFA	Metabolic flux analysis
NADH	Nicotinamide adenine dinucleotide
NADPH	Nicotinamide adenosine dinucleotide phosphate
PHB	Poly-3-hydroxybutyrate
PLA	Poly(lactic acid)
SDS	Sodium dodecyl sulfonate

E. Martínez-Hernández (✉) · M. A. Amezcua Allieri · J. A. Aburto Anell
Biomass Conversion Division, Instituto Mexicano del Petróleo, Mexico City, Mexico
e-mail: emartinez@imp.mx

K. S. Ng · J. Sadhukhan
Centre for Environmental Strategy, University of Surrey, Guildford, UK

© Springer International Publishing AG, part of Springer Nature 2018
R. K. Sani, N. K. Rathinam (eds.), *Extremophilic Microbial Processing of Lignocellulosic Feedstocks to Biofuels, Value-Added Products, and Usable Power*,
https://doi.org/10.1007/978-3-319-74459-9_14

What Will You Learn from This Chapter?

- An overview of value-added production using extremophiles as well as the advantages and challenges for process development
- Process development using extremophiles for value-added products from wastes in a biorefinery concept
- A modeling framework that includes microorganism's metabolism, growth kinetics, and bioreactor models as well as process simulation
- Economic analysis and life cycle assessment and application to continuous production of poly-3-hydroxybutyrate (PHB) using the halophilic bacteria *Halomonas* sp.

14.1 Introduction

A biorefinery can be defined as a complex system for the sustainable processing of biomass by a systematic integration of physical, chemical, biochemical, and thermochemical processes to obtain a range of products such as chemicals, nutraceuticals, pharmaceuticals, polymers, and energy such as biofuels, heat, and power (Sadhukhan et al. 2014). By producing a mix of products through flexible and efficient processes, biorefineries have the potential to make biomass processing profitable. Biorefineries also represent a sustainable and low-pollution system alternative to petroleum processing. The projected market created throughout the entire value chain of biomass to value-added products in biorefineries is \$295 billion by 2020 (King 2010). However, biorefineries have been developed based on simple biofuel plants producing bioethanol or biodiesel and low-value coproducts such as dried distillers' grains with solubles (DDGS) or glycerol. Current first-generation biofuel plants use mainly food crops as feedstock that create socioeconomic conflicts such as the food vs. fuel debate, and they still use fossil resources for their energy and auxiliary raw material requirements. Indeed, the Mexican government limits the use of food crops such as maize and cereals for bioethanol fuel production to avoid this food vs. fuel concern (Diario Oficial 2008). With increasing concerns on climate change, resource scarcity, and food poverty, a shift to lignocellulosic biomass processing is required (Aburto et al. 2008).

In order to improve economics and sustainability, a truly integrated biorefining approach that allows utilization of wastes for resource circularity is much needed (Satchatippavarn et al. 2016). The use of lignocellulosic residues has been widely explored in the recent years as second-generation feedstock using a biochemical platform. However, pretreatment, conversion, and downstream processes still need extensive efficiency improvements to make it more attractive, thus making biorefinery products economically, environmentally, and socially sustainable. Several approaches have been applied to improve the efficiency and the environmental sustainability of biofuel production. On one hand, genetic and metabolic engineering to improve microorganism's performance in converting lignocellulose into products

has been extensively explored in the recent years. On the other hand, process engineering tools have been developed for on-site energy and raw material supply and value-added production (Martinez-Hernandez et al. 2013b; Sadhukhan et al. 2014) as well as for economic and environmental assessment (Martinez-Hernandez et al. 2013a). Although the choice of microorganism and growing conditions will affect the ideal pretreatment and downstream processing, the two approaches are often carried out separately. Furthermore, current microorganisms are designed to grow in carefully controlled mild conditions that require more processing steps, which increase both capital and operating costs.

With the aim to address the challenges of processing wastes with minimum requirements and process steps and in a wide range of conditions, the use of extremophiles has been recently proposed (González-García et al. 2013; Bhalla et al. 2013; Bosma et al. 2013; Zambare et al. 2011; Ramírez et al. 2006). All these organisms grow at unusual and extreme conditions that prevent microbial contamination and may have some advantages for processing feedstocks and downstream recovery and purification of products. For example, extremophiles growing at high temperatures could be used for ethanol production at a temperature at which ethanol would evaporate, thus avoiding product inhibition and easing purification (Zambare et al. 2011). Another example of value-added product from extremophiles is the production of poly-3-hydroxybutyrate (PHB) using halophilic bacteria (Lorantfy et al. 2014; Garcia-Lillo and Rodriguez-Valera 1990). Halophilic bacteria grow at high-salinity conditions and lyse when salinity decreases, thus releasing PHB, which is an internal constituent of cell biomass. The exploration of the potential of extremophiles for chemical production has just emerged, and more studies are needed to achieve high conversion efficiency, productivities, and economic profitability. For several extremophiles, genetic and process engineering tools are already available, but these are mostly used for the optimization of ethanol production. Engineering organisms and processes for the conversion of wastes into chemicals would be an important next step. Interesting questions for designing processes using extremophiles are the implication for suitable product recovery and purification steps, equipment materials, energy consumption, and environmental impact.

This chapter presents a framework for modeling, simulation, and optimization tools for process development using extremophiles for sustainable production of value-added products from wastes in a biorefinery concept. This is crucial for developing extremophiles such as industrial platform organisms and optimizing biorefinery processes. This chapter starts with an overview of value-added production using extremophiles as well as the advantages and challenges for process development. Then, the various elements of the modeling framework include microorganism's metabolic model, growth kinetics and bioreactor model, process simulation, and economic and environmental impact analysis. These are illustrated with examples for PHB production using the halophilic bacteria *Halomonas* sp. (strain KM-1 recently studied by Jin et al. 2013). A biorefinery process scheme for extremophilic conversion of sugarcane bagasse into PHB is developed under the Mexican context. Furthermore, economic and life cycle analysis and implications for

whole process optimization are devised in order to guide future research on biorefinery process development based on extremophiles.

14.2 Extremophile Processing for Value-Added Production from Waste

Examples of some extremophile types and their implications for processing in terms of advantages and challenges are summarized in Table 14.1. Main value-added products being explored by using extremophiles include hydrogen, ethanol, lactic acid, ectoine, and poly-3-hydroxybutyrate (PHB) (Bosma et al. 2013).

Table 14.2 shows examples of extremophile processing of waste for value-added production. Lactic acid is a value-added chemical with a market demand of 500 kton and current production of 300–400 kton per year (NNFCC 2016). Lactic acid is the building block for polylactic acid (PLA) and other products. The conventional production process uses calcium hydroxide to neutralize the fermentation broth and precipitate calcium lactate. The acid is then recovered by acidification with sulfuric acid which produces gypsum (CaSO_4) which has low commercial value and needs to be disposed of. Development of microorganisms which can tolerate acidic conditions (lower pH) can reduce the unit cost of recovery and purification using an extraction process (Kumar et al. 2006). In this sense, acid-tolerant thermophilic

Table 14.1 Extremophile types and implications for the biorefinery process

Extremophile type	Example	Advantages	Challenge
Thermophilic	<i>Thermoanaerobacter</i> ($T > 70\text{ }^\circ\text{C}$) for ethanol production (Georgieva et al. 2007)	Easier recovery of volatile products such as ethanol Lower product inhibition Sterilization may not be required and microbial contamination is avoided	Higher fermentation temperatures may imply higher utility consumption for heating and cooling
Acidophilic	Thermophilic <i>Acidophilic Bacillus</i> sp., pH = 5.0 and $T = 55\text{ }^\circ\text{C}$ for lactic acid production (Patel et al. 2005)	Lower neutralization agent required, thus less salt waste	Anticorrosive materials needed for equipment
Halophilic	<i>Halomonas</i> sp. and <i>Haloferax mediterranei</i> (salinity 3–15% weight/volume basis) for PHB production (Jin et al. 2013; Rathi et al. 2013)	Easier recovery of intracellular PHB product by osmotic lysis leads to less processing steps	Anticorrosive materials needed for equipment Salts may need to be discarded

Table 14.2 Examples of extremophile processing of waste for value-added production

Feedstock	Process and product	Microorganism and conditions	Reference
Glycerol	Fermentation for acetate and carotenoids	<i>Haloferax mediterranei</i> , 37 °C and hypersaline (min 10% weight and salt concentration)	Lorantfy et al. (2014)
Sugarcane bagasse	Simultaneous saccharification and fermentation (SSF) to produce L(+)-lactic acid	Thermophilic <i>Acidophilic Bacillus</i> sp. (36D1), pH = 5.0 and 55 °C	Patel et al. (2005)
Corn stover and prairie cord grass	Hydrolysis and consolidated bioprocessing to ethanol	<i>Geobacillus</i> sp. R7, 70 °C and 15–20% solid content	Zambare et al. (2011)
Oil palm empty fruit bunch	Fermentation to lactic acid	<i>Bacillus coagulans</i> JI12 50 °C	Ye et al. (2014)
Sugarcane bagasse	Fermentation to lactic acid	<i>Bacillus</i> sp., 50 °C and pH = 5	Patel et al. (2004)
Sugarcane molasses	Batch fermentation to lactic acid	<i>Lactobacillus delbrueckii</i>	Dumbrepatil et al. (2008)
Whey	Fermentation to PHB	<i>Haloferax mediterranei</i>	Koller et al. (2008)

bacteria such as *Bacillus coagulans* could help to produce L-lactic acid from lignocellulose sugars in a more environmentally friendly manner.

Halophilic bacteria *Haloferax mediterranei* was studied by Garcia-Lillo and Rodriguez-Valera (1990) for the production of poly-3-hydroxybutyrate (PHB). The minimum of 90 g L⁻¹ of NaCl is required for growth and tolerance is up to 300 g L⁻¹. This strain accumulates PHB during exponential growth; thus, using one bioreactor stage was feasible for continuous production. Despite the advantages of halophilic bacteria for PHB production (e.g., solvent-free recovery and purification, can use inexpensive carbon source), several drawbacks exist. High salinity requires expensive bioreactor materials. Recycling of the salts and nutrients may be needed to avoid environmental problems due to waste disposal. In this chapter, the use of a recently studied strain of *Halomonas* sp. for a biorefinery concept producing PHB polymer is modeled and analyzed as follows.

14.3 Modeling a Biorefinery for PHB Production Based on Extremophile Processing

From a process systems engineering perspective, a biorefinery can be viewed as a multilayer as shown in the onion model in Fig. 14.1. This figure illustrates the various modeling and optimization tools and objectives depending on the layer. A holistic view is encouraged in order to develop any new biorefinery concept based on extremophile processing, and therefore in applying these tools, there should be

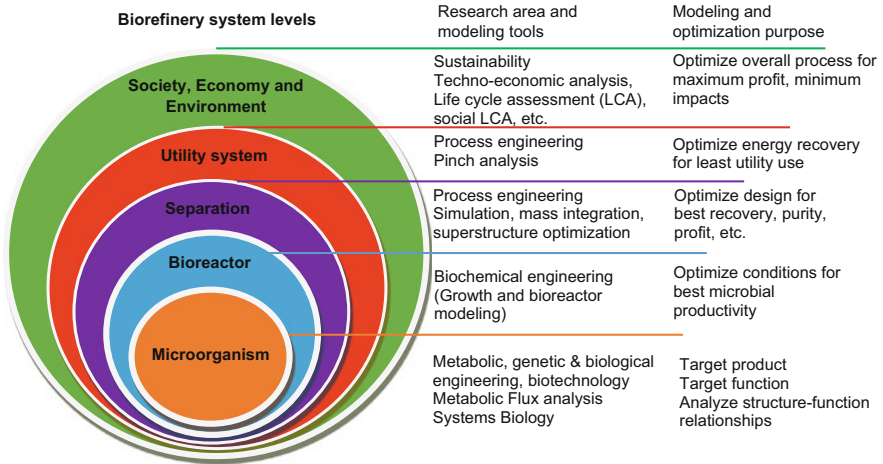


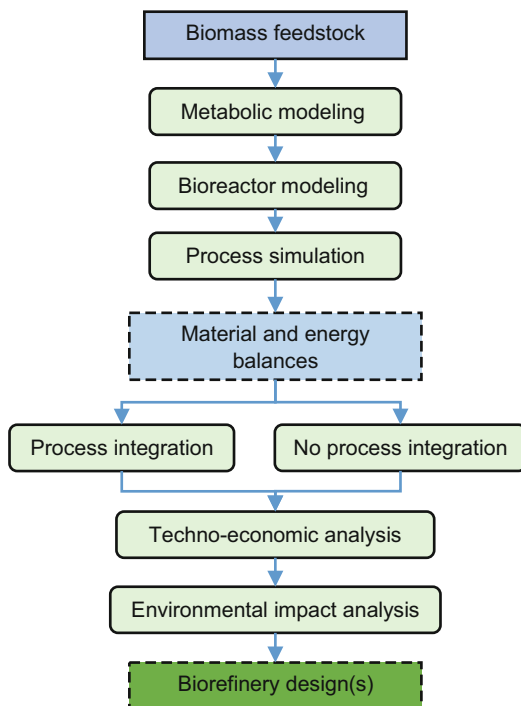
Fig. 14.1 Onion model of biorefinery system and the modeling tools and optimization purposes at each level

feedback between and across the various levels. The basic steps of the modeling framework illustrated in this book chapter are shown in Fig. 14.2. The framework offers a tool for accelerating biorefinery process development and is illustrated for PHB production. Modeling of PHB production has been widely studied in the literature (Koller et al. 2006; Koller and Muhr 2014) with special focus on bioreactor modeling but not the whole process and rarely using halophilic bacteria (Dotsch et al. 2008).

14.3.1 *Metabolic Modeling: Microorganism's Cells as the Core of Biochemical Processes*

A few decades ago, the reactions occurring at the cellular level in a bioreactor were traditionally taken somewhat as a black box due to the simplicity for parametrization and practicality for design. As such, the core of the process was simply the bioreactor, and only the macroscopic nature of this process unit was considered for modeling and optimization. With the advancement of metabolic and genetic engineering as well as computational capabilities, the approach is shifting toward viewing not the reactor vessel per se as the core of a biochemical process but the microorganism cells. It is in the cells where all the reactions that transform raw material into products actually occur, and, as such, the microorganism cells are the micro-reactors that need to be understood first to optimize a biochemical process. To this end, metabolic engineering has largely contributed with mathematical modeling of biochemical reaction pathways or networks within microorganism cells, thus

Fig. 14.2 Modeling framework for biorefinery process development



helping to understand the relation between metabolism, culture conditions, and the productivity.

The analysis of the reaction pathways leading to each of the metabolism products and biomass constituents is called metabolic flux analysis (MFA). MFA is a mathematical modeling tool used to target reactions, enzymes, and genes that enhance a desired product or inhibit an undesirable by-product (Xu et al. 2008). This information then is passed on to genetics which can then target enzymes, chromosomes, and genes to engineer a microorganism to deploy certain functionality. Another tool is the metabolic balance, used to determine macroscopic parameters used in the modeling of bioreactors, thus leading to a multiscale model. Metabolic modeling requires more details about what is going inside the cells that requires specialized experimental techniques. Furthermore, the modeling does not consider spatial and temporal variations that may occur in a bioreactor. However, MFA is becoming more common in developing a bioprocess and will definitely play a role in the biorefineries based on the biochemical platform using extremophiles.

The construction of a metabolic model was formalized by Stephanopoulos et al. (1998). The model illustrated here involves the representation of the stoichiometry and kinetics of metabolic reactions in matrices and solving the resulting equation system in order to find the macroscopic specific yield coefficients. The basic steps can be summarized and illustrated as follows for halophilic bacteria producing PHB from glucose.

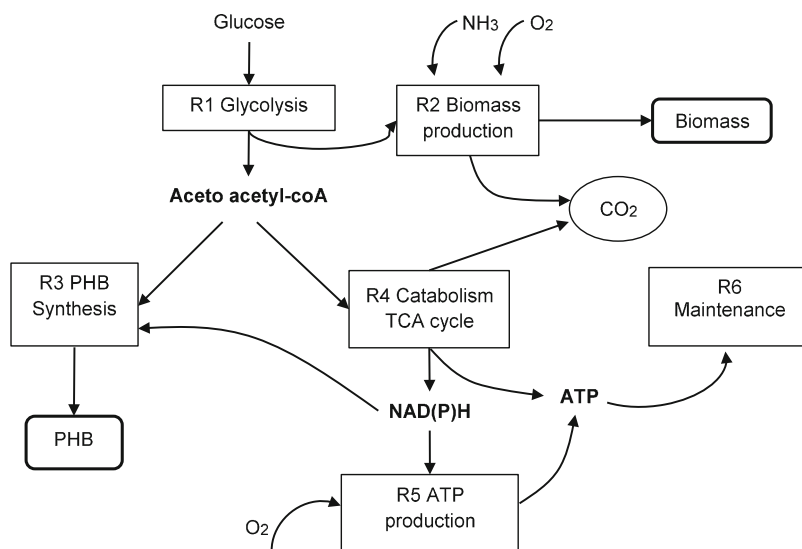


Fig. 14.3 Simplified metabolic model for PHB production from *Halomonas* sp.

1. Identify the reactions and chemical species participating (consumed or produced) in the metabolic pathways of interest.

The simplified metabolic pathway for PHB production in the halophilic bacteria *Halomonas* sp. KM-1 (Jin et al. 2013) is shown in Fig. 14.3. Four types of species can be distinguished: substrates, metabolic products, biomass constituents, and intracellular metabolites. The *substrate* is glucose which is the raw material to be metabolized by the glycolysis reaction pathway. During these and other internal reactions, intermediates and building blocks are produced as *intracellular metabolites*. Glycolysis produces the intermediate acetyl-CoA. This is further metabolized by two pathways: the tricarboxylic cycle (TCA) and the PHB synthesis pathway. The TCA cycle is a pathway to generate energy via NADH (nicotinamide adenine dinucleotide) and NADPH (nicotinamide adenosine dinucleotide phosphate) by aerobic organisms. From this cycle, *metabolic products* (e.g., succinate, acetate, and ethanol) are excreted to the culture medium by some microorganisms and can be recovered as products from the fermentation broth. PHB is rather a cell *biomass constituent* together with other macromolecules such as RNA, DNA, lipids, proteins, and carbohydrates. This means that the cells need to be broken down to recover PHB, and thus cells cannot be recycled as in other fermentation processes.

Jin et al. (2013) identified 53 metabolites for *Halomonas* sp. The authors found that accelerating the TCA cycle produces the NADPH required for the PHB synthesis pathway as a coenzyme for the conversion of acetoacetyl-CoA into (R)-3-hydroxybutyryl-CoA (3-HB-CoA). This 3-HB-CoA is then converted into PHB. There could be hundreds of reactions occurring during microbial growth, but it would not be possible to include all for a metabolic model, as solving the system would be computationally expensive. The discrimination of which reactions to

Table 14.3 Metabolic model for PHB production

Reaction	Reaction equation
R1 Glucose conversion to acetyl-CoA	$C_6H_{12}O_6 \rightarrow \text{AcetylCoA} + 2\text{NAD(P)H} + 0.5\text{ATP} + \text{CO}_2$
R2 Biomass production (net reaction from glucose via acetyl-CoA)	$(1 + a)C_6H_{12}O_6 + \frac{1}{5}NH_3 + \left(\frac{2a-1}{4}\right)O_2 \rightarrow CH_{1.74}O_{0.46}N_{0.19} + aCO_2$
R3 PHB synthesis from acetyl-CoA	$2\text{AcetylCoA} + \text{NAD(P)H} + 0.5\text{ATP} \rightarrow \text{PHB}$
R4 Acetyl-CoA catabolism in the TCA cycle	$\text{AcetylCoA} \rightarrow 4\text{NAD(P)H} + \text{ATP} + 2\text{CO}_2$
R5 ATP production	$\text{NAD(P)H} + 0.5O_2 \rightarrow \delta\text{ATP}$
R6 ATP use for maintenance (nongrowth associated)	$-\text{ATP} = 0$

include is assisted by considering what is called the *relaxation time* and comparing with the time of the macroscopic process. This is the time that a reaction would take to complete when approximated as a first-order reaction (Stephanopoulos et al. 1998). For example, any process happening at slower rate than cell growth in a fermentation process can be neglected (e.g., mutations). Another basic concept that helps to simplify the metabolic model construction is the pseudo-steady-state assumption for very fast reactions (e.g., enzymatic catalysis). Thus, by assuming steady state, the intermediates are considered not to accumulate as they are consumed and generated fast. For illustration purposes, only the reactions shown in Fig. 14.3 will be used.

2. Construct matrix of reaction stoichiometry. This involves first balancing the basic metabolic reactions and then representing the resulting algebraic equation systems in a matrix to find the missing stoichiometric coefficients.

Table 14.3 shows the six reactions in the simplified metabolic model. Note that the notation NAD(P)H means either NADH or NADPH can participate, and to further simplify the exercise, they are lumped in a single pool of reducing species (Stephanopoulos et al. 1998).

The chemical stoichiometry can be represented by:

$$AS + BP + CX + DM = 0 \quad (14.1)$$

where A contains the coefficients for the substrates, B those for products, C for biomass constituents, and D for intracellular metabolites. These matrices represent the J reactions in the rows and the species I in the columns so that the coefficient v_{ij} in each element shows the coefficient of a species i in reaction j . The vectors S , P , X , and M represent the concentrations of the species. For the PHB production model, Eq. (14.1) can be expanded to:

$$\begin{aligned}
& \begin{bmatrix} -1 & 0 & 0 \\ -(1+a) & -\left(\frac{2a-1}{4}\right) & -0.2 \\ 0 & 0 & 0 \\ 0 & 0 & 0 \\ 0 & -0.5 & 0 \\ 0 & 0 & 0 \end{bmatrix} \begin{bmatrix} S_G \\ S_{O_2} \\ S_{NH_3} \end{bmatrix} + \begin{bmatrix} 1 \\ a \\ 0 \\ 2 \\ 0 \\ 0 \end{bmatrix} [P_{CO_2}] \\
& + \begin{bmatrix} 0 & 0 \\ 1 & 0 \\ 0 & 1 \\ 0 & 0 \\ 0 & 0 \\ 0 & 0 \end{bmatrix} \begin{bmatrix} X_B \\ X_{PHB} \end{bmatrix} + \begin{bmatrix} 1 & 2 & 0.5 \\ 0 & 0 & 0 \\ -2 & -1 & -0.5 \\ -1 & 4 & 1 \\ 0 & -1 & \delta \\ 0 & 0 & -1 \end{bmatrix} \begin{bmatrix} M_{AcCoA} \\ M_{NAD(P)H} \\ M_{ATP} \end{bmatrix} \\
& = \begin{bmatrix} 0 \\ 0 \\ 0 \\ 0 \\ 0 \\ 0 \end{bmatrix} \tag{14.2}
\end{aligned}$$

where concentrations of the three substrates are denoted by S_G , S_{O_2} , and S_{NH_3} for glucose, oxygen, and ammonia, respectively, those for CO_2 product by P_{CO_2} , and the biomass constituents by X_B and X_{PHB} and the intracellular metabolites as M_{AcCoA} , $M_{NAD(P)H}$, and M_{ATP} . By convention, v_{ij} is negative for reactants and positive for products. Assuming that a and δ are known, there are a total of nine variables and six equations, resulting in a degree of freedom equal to three.

3. Formulate reaction rate expressions and apply the pseudo-steady-state assumption to intracellular metabolite production rates in order to have a fully determined algebraic equation system.

In this step, the production rates for each species are formulated from the reaction rates. This is to express production or consumption rates using reactions that can be easily measured experimentally. In general, the production rates of biomass, PHB, and CO_2 or consumption of glucose and other nutrients is measurable. The matrix R containing the reaction rates is related to each specie's production or consumption rate r_i by their respective coefficient matrix as:

$$R_i = K^T \times R \tag{14.3}$$

where R_i is a one column matrix containing the production rates of substrates r_G , r_{O_2} , and r_{NH_3} , metabolite products r_{CO_2} , biomass constituents r_B and r_{PHB} , or intracellular metabolites r_{AcCoA} , $r_{NAD(P)H}$, and r_{ATP} . The matrix R contains the rates r_1 to r_6 for the reactions 1–6 in the metabolic model (Table 14.3 in this example). K^T is the transpose matrix of the corresponding coefficient matrix (A , B , C , or D from Eq. 14.2). The pseudo-steady state is then applied for the intracellular metabolites,

so that their net consumption or production can be assumed equal to 0. For the matrix M Eq. (14.2) containing r_{AcCoA} , $r_{\text{NAD(P)H}}$, and r_{ATP} , Eq. (14.3) gives:

$$\begin{bmatrix} r_{\text{AcCoA}} \\ r_{\text{NAD(P)H}} \\ r_{\text{ATP}} \end{bmatrix} = \begin{bmatrix} 1 & 2 & 0.5 \\ 0 & 0 & 0 \\ -2 & -1 & -0.5 \\ -1 & 4 & 1 \\ 0 & -1 & \delta \\ 0 & 0 & -1 \end{bmatrix}^T \times \begin{bmatrix} r_1 \\ r_2 \\ r_3 \\ r_4 \\ r_5 \\ r_6 \end{bmatrix} = \begin{bmatrix} 0 \\ 0 \\ 0 \end{bmatrix} \quad (14.4)$$

This results in the following expressions:

$$\begin{pmatrix} r_{\text{AcCoA}} \\ r_{\text{NADPH}} \\ r_{\text{ATP}} \end{pmatrix} = \begin{pmatrix} r_1 - 2 \cdot r_3 - r_4 \\ 2 \cdot r_1 - r_3 + 4 \cdot r_4 - r_5 \\ 0.5 \cdot r_1 - 0.5 \cdot r_3 + r_4 + \delta \cdot r_5 - r_6 \end{pmatrix} = \begin{pmatrix} 0 \\ 0 \\ 0 \end{pmatrix} \quad (14.5)$$

Applying Eq. (14.3) to other species (this time without the steady-state assumption), the following expressions are obtained:

$$\begin{pmatrix} r_G \\ r_{\text{O}_2} \\ r_{\text{NH}_3} \\ r_{\text{CO}_2} \\ r_B \\ r_{\text{PHB}} \end{pmatrix} = \begin{bmatrix} -r_1 - r_2 \cdot (1 + a) \\ -0.5 \cdot r_5 - r_2 \cdot \left(\frac{2a - 1}{4}\right) \\ -0.2 \cdot r_2 \\ r_1 + 2 \cdot r_4 + a \cdot r_2 \\ r_2 \\ r_3 \end{bmatrix} \quad (14.6)$$

ATP consumed for nongrowth associated maintenance can be correlated to the cell biomass by the specific maintenance factor m_{ATP} as:

$$r_6 = m_{\text{ATP}} X_B \quad (14.7)$$

Thus, the equation system is now completely determined, and Eqs. (14.6 and 14.7) can be combined with Eq. (14.5) to derive the expressions for the measurable reaction rates:

$$\begin{pmatrix} -r_G \\ -r_{\text{O}_2} \\ r_{\text{CO}_2} \end{pmatrix} = \begin{bmatrix} \frac{0.667}{1 + 4\delta} \cdot m_{\text{ATP}} \cdot X_B + \frac{6\delta + 1.667}{1 + 4\delta} \cdot r_{\text{PHB}} + \frac{a + 4\delta + 4a\delta + 1}{1 + 4\delta} \cdot r_B \\ \frac{2m_{\text{ATP}} \cdot X_B}{1 + 4\delta} + \frac{0.5 \cdot r_{\text{PHB}}}{1 + 4\delta} + \frac{(2a - 1) \cdot r_B}{4} \\ \frac{2.667}{1 + 4\delta} \cdot m_{\text{ATP}} \cdot X_B + \frac{8\delta + 2.667}{1 + 4\delta} \cdot r_{\text{PHB}} + a \cdot r_B \end{bmatrix} \quad (14.8)$$

4. Find yield coefficients. The yield coefficients are the ratio of mass of species i formed per mass of species i' consumed. For example, the yield coefficients are related to the specific substrate consumption rate (q_s) using the Herbert-Pirt equation

for substrate distribution toward specific growth (μ), specific product formation (q_P), and maintenance (m_S):

$$-q_S = m_S + \frac{q_P}{Y_{PS}^{\max}} + \frac{\mu}{Y_{XS}^{\max}} \quad (14.9)$$

From Eq. (14.8), the specific rates for glucose, oxygen, and CO₂ can be obtained by dividing the biomass concentration X_B , resulting in the following Herbert-Pirt relationships:

$$\begin{pmatrix} -q_G \\ -q_{O_2} \\ q_{CO_2} \end{pmatrix} = \begin{bmatrix} \frac{0.667}{1+4\delta} \cdot m_{ATP} + \frac{6\delta+1.667}{1+4\delta} \cdot q_{PHB} + \frac{a+4\delta+4a\delta+1}{1+4\delta} \cdot \mu_B \\ \frac{2m_{ATP}}{1+4\delta} + \frac{0.5 \cdot q_{PHB}}{1+4\delta} + \frac{(2a-1) \cdot \mu_B}{4} \\ \frac{2.667}{1+4\delta} \cdot m_{ATP} + \frac{8\delta+2.667}{1+4\delta} \cdot q_{PHB} + a \cdot r_B \end{bmatrix} \quad (14.10)$$

By inspection of the general form in Eq. (14.9) and the first expression in Eq. (14.10), the maximum theoretical yields of biomass and PHB from glucose are:

$$Y_{XS}^{\max} = (1+4\delta)/(a+4\delta+4a\delta+1) \quad (14.11)$$

$$Y_{PS}^{\max} = (1+4\delta)/(6\delta+1.667) \quad (14.12)$$

Assuming $\delta = 3$, the values are $Y_{XS}^{\max} = 0.5 \text{ g g}^{-1}$ and $Y_{PS}^{\max} = 0.66 \text{ g g}^{-1}$. These values can then be compared with those reported in the literature but may need to be fine-tuned using experimentation and macroscopic bioreactor models. These yield coefficients will appear when the development of mass balances in bioreactors as shown later. The next sections of the modeling framework are based on the materials presented by Sadhukhan et al. (2014) for biorefinery process design, integration, and sustainability.

14.3.2 Growth Kinetics and Bioreactor Modeling

Kinetic models allow the prediction of microorganism's performance and serve as the basis for bioreactor modeling, design, and scale-up. Kinetic modeling involves experimentation from small-scale reactor experimentations in order to obtain model parameters. The dynamics of microorganism growth comprises a lag phase, an exponential phase, a stationary phase, and a death phase. Different products may be predominant at different stages. For example, PHB accumulation occurs mainly in the stationary phase, while the growth of microorganism cells occurs mainly in the exponential phase. Thus, a strategy used in PHB production is a two-stage reaction where growth happens in the first reactor and PHB accumulation in the second

reactor. This system potentially improves substrate conversion, yield, and also PHB content in the cell biomass, thus improving productivity.

14.3.2.1 Specific Growth Constant and Monod Equation

The kinetic parameters are usually obtained from the exponential phase of growth during batch experiments. In a batch reactor, there is no continuous input or output flows. If growth inhibition conditions are avoided during experimentation and mortality and maintenance are neglected, as they are much slower than growth in the exponential phase, then the rate of cell biomass growth during the exponential phase can be written as:

$$\frac{dX}{dt} = \mu X \quad (14.13)$$

where X is the total cell biomass concentration (including PHB accumulated inside the cells), μ is the specific growth rate as introduced in the previous section, and t is time. Integration of Eq. (14.13) from concentration X_1 at $t = t_1$ and X_2 at time t_2 results in the following form:

$$\ln(X_2) = \mu t + \ln(X_1) \quad (14.14)$$

Thus, it is possible to determine the value of μ from the slope of the line obtained by plotting the values of the logarithm vs. time.

Growth data extracted for *Halomonas* sp. KM-1 is shown in Table 14.4. The values of μ can be graphically determined from the linear fit shown in Fig. 14.4 as $\mu_1 = 0.2245 \text{ h}^{-1}$ and $\mu_2 = 0.2316 \text{ h}^{-1}$ for the initial glucose concentrations of 50 and 100 g L^{-1} , respectively.

Biomass growth is affected by several factors such as temperature, product, and substrate inhibition. The most common model for microorganism's growth used to capture such effects is the Monod kinetic equation. When describing the growth of a single culture limited by substrate concentration S , the Monod equation is written as:

$$\mu = \frac{\mu_{\max, S} S}{K_S + S} \quad (14.15)$$

Table 14.4 Growth data for *Halomonas* sp. KM-1 (Jin et al. 2013) at two different initial substrate concentrations

S1 = 50 g L^{-1}			S2 = 100 g L^{-1}		
Time (h)	X	S	Time (h)	X	S
10	3.5	35.89	12	3.559	83.47
12	4.26	32.78	14	5.69	70.29
14	7.7	25.1	15	8.03	64.44
15.2	10.9	21.99	18	14.58	44.07

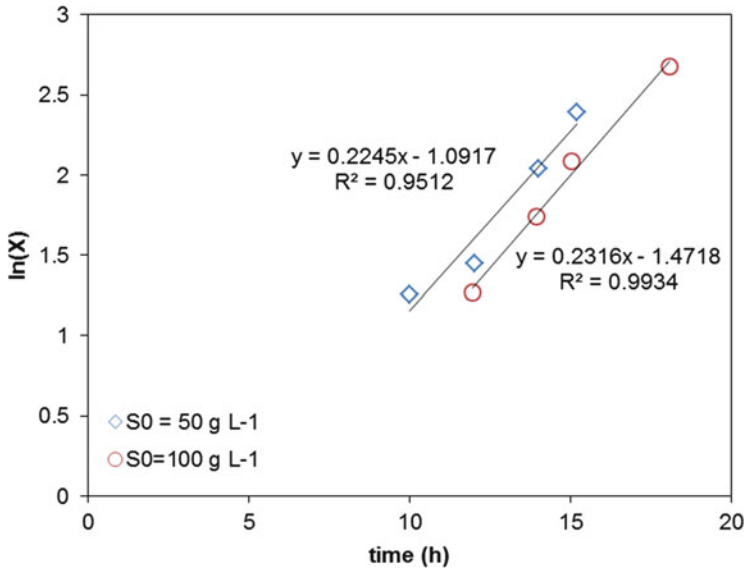


Fig. 14.4 Plot of $\ln(X)$ vs. time for two different initial concentrations (blue diamond: 50 g L^{-1} , red circle: 100 g L^{-1}) to find the specific growth rate of *Halomonas* sp. KM-1

where $\mu_{\max,S}$ is the maximum achievable growth rate and h^{-1} under the influence of substrate concentration. K_S is the saturation constant. This assumes that all the other factors are in optimum conditions. The parameters μ_{\max} and K_S can be estimated from the specific growth rate as a function of substrate concentrations. From Table 14.4, two data points are available for different initial substrate concentrations (S1 and S2). Therefore, two Monod equations can be formulated using Eq. (14.15). From the known values previously found for μ_1 and μ_2 , such equations can be solved to obtain $\mu_{\max,S} = 0.24 \text{ h}^{-1}$ and $K_S = 3.27 \text{ g L}^{-1}$. These values are comparable with values reported in the literature for other halophilic bacteria (e.g., $\mu_{\max,S} = 0.39$ and $K_S = 2.98$ for *H. mediterranei* (Koller et al. 2006).

When more data points are available, a better estimate could be obtained by linearizing Eq. (14.15). The resulting equation is the well-known Lineweaver-Burk equation, which allows obtaining μ_{\max} and K_S from a plot of $(1/\mu)$ vs $(1/S)$:

$$\frac{1}{\mu} = \frac{K_S}{\mu_{\max,S}} \frac{1}{S} + \frac{1}{\mu_{\max,S}} \quad (14.16)$$

This simple form of the Monod equation can be extended to include other fitting parameters. There could also be one Monod equation for each substrate. For example, the following model has been proposed for the effect of saline concentration Z on specific growth for halophilic bacteria (Dotsch et al. 2008):

$$\mu = \frac{\mu_{\max, Z} Z}{K_Z + Z + Z^2/k_1 + Z^3/k_2} \quad (14.17)$$

where $\mu_{\max, Z}$ is defined similarly to $\mu_{\max, S}$ and k_1 and k_2 are additional parameters.

14.3.2.2 Bioreactor Modeling

Batch reactors are one of the major reactors used both experimentally and industrially for biochemical production. The main advantage of batch reactors is that high product concentrations can be obtained. A variety of the batch reactor is the fed-batch reactor where a substrate or nutrient is fed periodically when there is inhibition to high concentrations or when a deficiency of nutrients favors the metabolism toward a desirable product. However, in order to improve process economics, a continuous reactor system can be used. High productivity, but lower concentrations, is achieved in continuous reactors. Dilution makes separation less efficient and may require more downstream processing steps. Thus, the trade-offs between productivity and purity of the product need to be carefully evaluated.

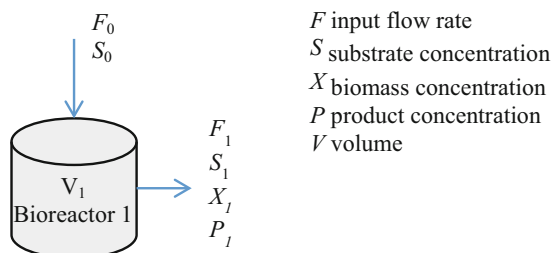
PHB production in a continuous process is desirable in order to improve process economics and also has consistency in the quality and properties of the polymer. Thus, this section will develop a model for an ideal continuously stirred tank reactor or CSTR as shown in Fig. 14.5. This reactor model allows assuming a homogeneous system and steady-state operation.

A CSTR reactor is modeled as follows. First, the mass balance for each component of interest is formulated, biomass and PHB in the case shown here. Remember that PHB is part of the internal cell biomass, but here the balance is done separately for PHB and the residual biomass (i.e., total biomass – PHB). The component mass balance has this general form: accumulation = input – output + generation – consumption (or death in case of microorganisms). Using the symbols in Fig. 14.5, cell biomass balance around the first reactor volume V_1 can be expressed as:

$$V_1 \frac{dX_1}{dt} = F_0 X_0 - F_1 X_1 + \mu_1 X_1 V_1 - k_d X_1 V_1 \quad (14.18)$$

Several assumptions can be made to simplify this expression such as constant volume, no biomass in the feed flow ($F_0 X_0 = 0$), and that the death rate can be

Fig. 14.5 Scheme showing the variables for modeling a continuous bioreactor for PHB production



F input flow rate
 S substrate concentration
 X biomass concentration
 P product concentration
 V volume

neglected assuming it is much smaller than growth ($k_d \ll \mu_1$). Dividing by V_1 , Eq. (14.18) is reduced to:

$$\frac{dX_1}{dt} = (\mu_1 - D_1)X_1 \quad (14.19)$$

where D_1 is known as the dilution rate equal to F_1/V_1 . Now, CSTR reactors reach a point in time where concentrations are constant; therefore it can be found that at steady state:

$$\mu_1 = D_1 \quad (14.20)$$

This suggests that to achieve the maximum growth, the dilution rate at which a CSTR bioreactor operates should be tuned to the specific growth rate. Note that parameters for the Monod equation can be also found using a CSTR reactor by varying the dilution rate at constant fermentation volume.

The reactor operates under limiting substrate; therefore, a mass balance for glucose can be written as:

$$V_1 \frac{dS_1}{dt} = F_0S_0 - F_1S_1 - \frac{1}{Y_{XS}^{\max}} \mu_1 X_1 V_1 - m_s X_1 V_1 - \frac{1}{Y_{PS}^{\max}} q_{PHB} X_1 V_1 \quad (14.21)$$

At steady state and neglecting PHB generation, as it is much slower than the biomass growth under nitrogen rich conditions ($\frac{q_{PHB} X_1}{Y_{PS}^{\max}} \ll D(S_0 - S_1)$), and dividing by V_1 , Eq. (14.21) simplifies to:

$$D_1(S_0 - S_1) = \frac{1}{Y_{XS}^{\max}} \mu_1 X_1 + m_s X_1 \quad (14.22)$$

Dividing by μ_1 and biomass concentration X_1 , and since at steady state $\mu_1 = D_1$, Eq. (14.22) becomes:

$$\frac{1}{Y_{XS}} = \frac{1}{Y_{XS}^{\max}} + \frac{m_s}{\mu_1} \quad (14.23)$$

where Y_{XS} is the overall yield of biomass from glucose and Y_{XS}^{\max} is the theoretical yield coefficient of biomass from glucose (as in Eq. 14.9). With known experimental yield data, the values of Y_{XS}^{\max} and m_s can be obtained and used to calibrate the metabolic model studied in Sect. 14.3.1.

Finally, the product mass balance can be written as follows:

$$V_1 \frac{dP_1}{dt} = F_0P_0 - F_1P_1 + q_{PHB} X_1 V_1 \quad (14.24)$$

At steady state and with $P_0 = 0$:

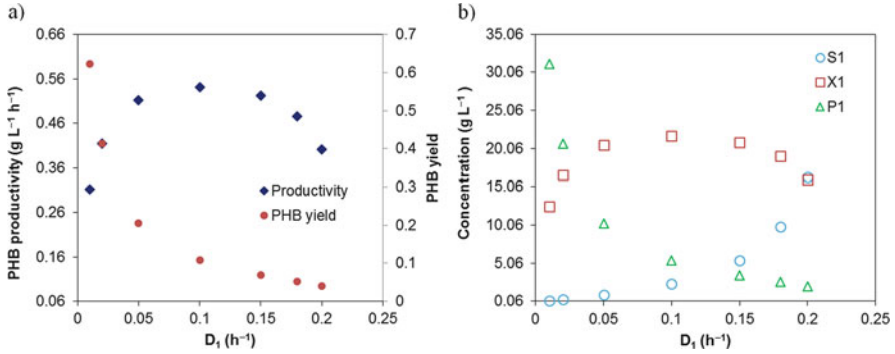


Fig. 14.6 Optimization of PHB production at various dilution rates (D_1) in one CSTR showing (a) blue diamond: productivity and red circle: yields and (b) blue circle: concentrations of substrate (S1), red square: residual biomass (X1), and green triangle: PHB (P1)

$$q_{\text{PHB}} = \frac{1}{X_1} D_1 P_1 \quad (14.25)$$

Thus, solving the equation system (Eqs. 14.20, 14.22, and 14.25), the values of outlet concentration of substrate, biomass, and PHB can be calculated for various dilution rates. Subsequently, the optimum D_1 for the maximum productivity P_{PHB} (g L⁻¹ h⁻¹) can be obtained. Productivity can be calculated as:

$$P_{\text{PHB}} = D_1 P_1 \quad (14.26)$$

Figure 14.6 shows the concentrations and values of productivity and PHB yield (kg PHB per kg glucose input) at different dilution rates after solving the mass balance equations using the parameters found previously for *Halomonas* sp.: $\mu_{\text{max}} = 0.24 \text{ h}^{-1}$, $K_S = 3.27 \text{ g L}^{-1}$, $m_S = 0.02 \text{ h}^{-1}$, $Y_{\text{XS}}^{\text{max}} = 0.5$, and $q_{\text{PHB}} = 0.025 \text{ h}^{-1}$. The initial glucose in a sugarcane bagasse hydrolysate was assumed to be concentrated up to 50 g L^{-1} . Note how the highest productivity is obtained at around $D_1 = 0.1 \text{ h}^{-1}$ with a PHB yield of 10.8% and a concentration of 5.41 g L^{-1} . The PHB content in biomass can be calculated as 20%. Thus, the residual biomass was 21.67 g L^{-1} and the total biomass (residual + PHB) is 27.1 g L^{-1} .

As mentioned previously, to improve yield and PHB concentration and content in biomass, the strategy used is a two-stage reactor system. Equations for the second bioreactor in the system can be derived in a similar way to the one shown here for the first reactor. However, as the second reactor operates with nitrogen limitation, the effect of nitrogen can be captured in the model by a Monod equation.

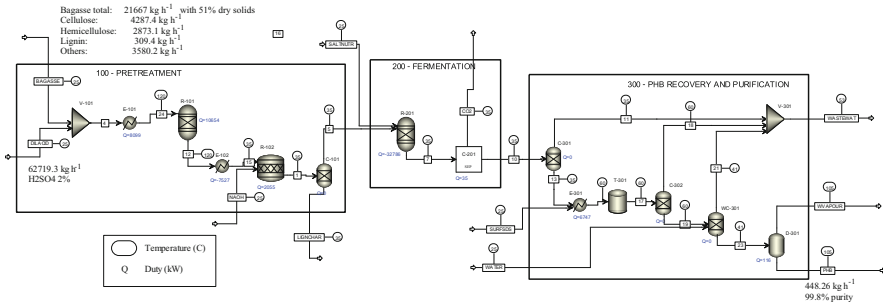


Fig. 14.7 Simulation flow sheet of PHB production process in a biorefinery using halophilic bacteria

14.3.3 Process Simulation of Extremophile-Based Process for PHB Production

PHB production using *Halomonas* sp. is analyzed in terms of its economics and greenhouse gas (GHG) emissions. The flow sheet simulated in the process simulator Aspen Plus® is shown in Fig. 14.7. The basis for the simulation is the production of 2000 t per year of PHB from sugarcane bagasse containing 51% of dry matter. The dry matter composition is 38.8% glucan, 23.5% xylan, 2.5% arabinan, 2.8% ash, and 32.4% lignin and others. The whole process consists of the following areas:

- A-100: Pretreatment. Bagasse is pretreated by diluting H_2SO_4 (2% mass basis) at 120 °C and followed by enzymatic saccharification. The whole pretreatment has been simulated as one unit R-101. Then, the hydrolysate is neutralized using NaOH in R-102. The lignin, ash, and char formed are then separated as solids by centrifugation in C-101, and sugars are recovered in the liquid stream which is then sent to the next area.
- A-200: Fermentation. The hydrolysate is then sent to fermenter R-201 for conversion of sugars into PHB, cell biomass, and CO_2 . The CO_2 from cell metabolism and respiration is vented out but could ideally be recovered for further conversion, thus avoiding process of GHG emissions. The fermentation broth is then sent to area A-300.
- A-300: PHB recovery and purification. Here, the broth passes through centrifuge C-301 to separate the total biomass containing the PHB from the liquid stream. Since PHB is a microorganisms' intracellular constituent, the cells need to be lysed, in order to recover this product. The main advantage of using halobacteria is that cells are easily lysed by a sudden change in salt concentration between the fermentation broth and pure water. The osmotic differential breaks down the cells and releases the PHB granules. The recovery and purification are thus simplified as no further treatment and no solvent are required, unlike the current typical process for PHB production with non-halophilic bacteria. Therefore, biomass treatment is carried out in T-301 as described. To improve recovery yield and

purity, sodium dodecyl sulfonate (SDS) solution at 0.1% (weight/volume basis) is used as the surfactant to assist the separation of the residual biomass from PHB granules (Rathi et al. 2013). The PHB granules are recovered from C-202 and is then washed and centrifuged to remove any remaining soluble components in WC-301. Afterward, the PHB granules are spray-dried in D-201 to obtain a mass purity of >98%. The use of the halophilic bacteria shows reduction of process steps and avoids using hazardous chemicals and solvents. Furthermore, the separation of the biomass from the liquid phase allows recycling of salts and nutrients required for the growth of halophilic bacteria. However, the use of high salinity would need corrosion-resistant equipment.

The overall process yield of PHB relative to bagasse was 2.1% despite using the optimum dilution rate (D_1) determined from the bioreactor modeling section. Thus, it is necessary to look at the whole picture in order to select the optimum D_1 at the process level and not only at the bioreactor or microorganism level. Thus, the process can still be optimized by selecting the appropriate dilution rate in the bioreactor. Another strategy would be the two-stage bioreactor system. But in order to decide the best option, some economic and environmental impact analysis might be required, as shown in the following sections.

14.3.4 Economic Analysis of PHB Production in a Extremophile-Based Biorefinery

Economic analysis was performed according to Sadhukhan et al. (2014), and the currency used was US dollars (\$). The plant operates only 4380 h per year while there is sugarcane available to obtain the bagasse. The bagasse price was 16 \$ t⁻¹, and the prices and costs were obtained for Mexico when information was available (Barrera et al. 2016). The biorefinery plant included an effluent treatment plant. Two cases were analyzed:

Case A: dilution rate $D = 0.1$ for maximum bioreactor productivity (Sect. 14.3.2.2).

The PHB yield in the bioreactor was 10.8%, the glucose conversion was 95.3%, and the PHB content in biomass was 20% with a productivity of 0.54 g L⁻¹ h⁻¹.

The overall PHB yield in respect to bagasse input was 2.1%.

Case B: dilution rate $D = 0.01$ for high PHB yield in the bioreactor = 62%. The glucose conversion was 99.7%, and the PHB content in biomass was 71.4% with a productivity of 0.31 g L⁻¹ h⁻¹. The overall PHB in respect to bagasse input was 11.9%. This case includes a combined heat and power (CHP) plant from solid residues.

The objective of the economic analysis was to analyze the minimum selling price for profitability. The discount rate was set at 10% and the plant lifetime was 15 years. Figure 14.8 shows the results of economic analysis. Figure 14.8a shows that capital costs contribute to total annual costs by up to 51%. The direct operation costs are

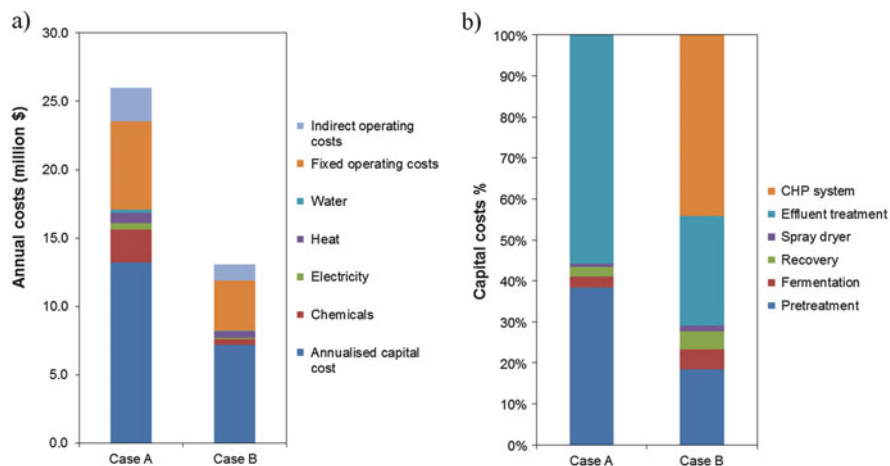


Fig. 14.8 (a) Annual operating cost and (b) capital cost contribution by various sections of the PHB production process for case A (low yield and no CHP plant) and case B (high yield and with CHP plant)

contributed mainly by chemicals (9% of total) and then energy (5% of total). Figure 14.9 shows that the minimum selling price for a positive netback from bagasse would need to be 13.76 \$ kg⁻¹ in case A. This would make PHB from halophiles not competitive with other production technologies and other biopolymers such as polylactide- and starch-based polymers with values reported in the range of 5–12 \$ kg⁻¹ (Mudliar et al. 2008; Choi and Lee 1997).

Figure 14.8 shows how the operating costs decrease by 50% in case B due to increased overall yield. Lower bagasse needs to be processed (for the same PHB production of 2000 t per year) and thus lower chemical requirements and lower effluents. When looking at hot spots in the capital costs in Fig. 14.8b, the effluent treatment had a high contribution in case A which is reduced significantly in case B. Furthermore, case B allowed the integration of a combined heat and power (CHP) plant using the solid residues to supply 80% of electricity and 34.5% of heat requirements. This on-site energy supply will have a positive effect on the environmental performance as shown in the next section. Sensitivity analysis in Fig. 14.9 showed that minimum selling price in case B is reduced to 7.05 \$ kg⁻¹. This price is within the range of values reported in the literature which means that PHB production from halophiles could be competitive for specialty applications. However, it would be difficult to compete as a commodity with petrochemical-based polymers, which prices are just around 1.2 \$ kg⁻¹ (e.g., low density polyethylene).

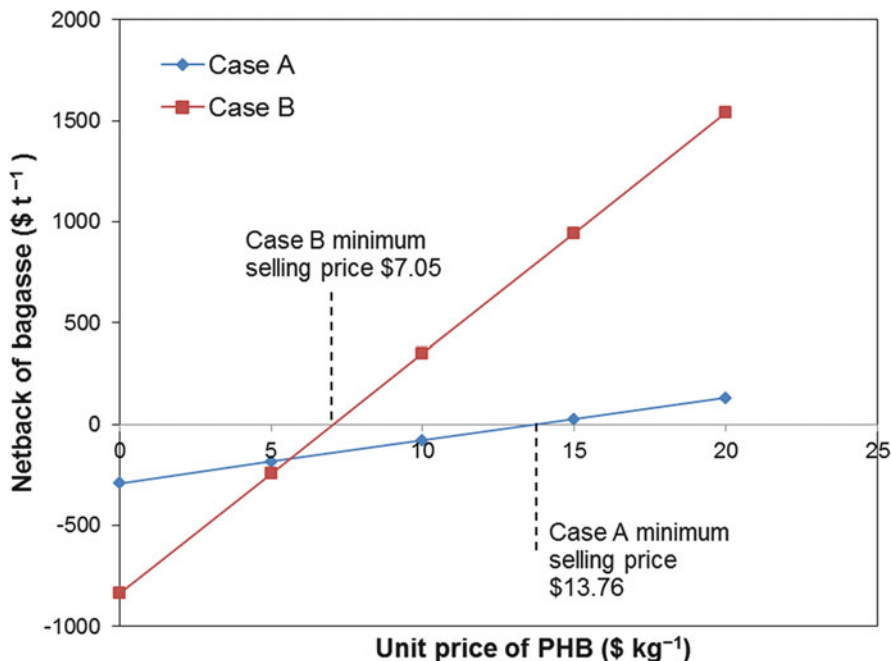


Fig. 14.9 Sensitivity analysis to determine minimum PHB selling price for positive netback in blue diamond: case A and red square: case B

14.3.5 Life Cycle Assessment (LCA) of PHB Production System

The LCA is a holistic and systematic environmental impact assessment tool in a standardized way and format for cradle to grave systems. According to the International Organization for Standards (ISO) 14040, 14041, and 14044, the LCA is carried out in four phases: goal and scope definition, inventory analysis, impact assessment, and interpretation (ISO 1997). All these phases are interdependent, as the result of one phase determines the execution of the next phase. Although LCA is a standard technique, it needs a practitioner's expertise to ensure that the system is correctly defined, inventories are robust, and impacts assessed and interpretations are comprehensive (Sadhukhan et al. 2014).

The LCA study follows these ISO guidelines, practical implementation of which has been discussed in Sadhukhan et al. (2014). The system boundary includes the direct, indirect, and embedded inputs and outputs. The inlet and outlet mass and energy flowrates of the system were extracted from the process modeling and simulation discussed in earlier sections. For each inlet or outlet flow, inventory data were extracted from ecoinvent 3.0 and characterized and aggregated for life cycle impacts in various categories using GaBi 6.0 (Thinkstep 2016). The most relevant and important impact characterizations for the system are global warming,

Table 14.5 Inlet and outlet raw material and energy flowrates of the system, for which inventory data were extracted from Ecoinvent 3.0, for cases A and B

Per kg PHB production	Case A (low yield, no CHP)	Case B (high yield, CHP)
Direct emission from the plant (i.e., CO ₂ emission from the fermenter), kg CO ₂	0.2125	0.2125
Quantity of raw materials causing indirect impacts of the plant		
Heat from combustion of natural gas, MJ	58.7791	
Sodium hydroxide, kg	2.2844	0.3977
Grid electricity, MJ	5.8950	
SDS, kg	0.5197	0.0521
Sodium chloride, kg	1.1434	0.1285
Sulfuric acid, kg	0.2798	0.0487
Make-up water, kg	131.7748	15.5924
Embedded or captured CO ₂ in PHB, kg CO ₂	-2.0465	-2.0465

acidification, eutrophication, freshwater aquatic ecotoxicity, human toxicity, and photochemical ozone creation potentials.

The direct greenhouse gas (GHG) emission from the PHB production process, indirect GHG emission due to sourcing of raw materials needed by the PHB production process, and embedded or sequestered carbon in PHB have been taken into account in the estimation of the life cycle global warming potential over 100 years (GWP). The inlet and outlet flowrates of the system, for which inventory data were extracted from Ecoinvent 3.0, are shown for cases A and B, in Table 14.5.

Case A gives a total of 7.0114 kg CO₂ equivalent GWP (per kg PHB) from the PHB production system with utilities sourced externally. However, if separated solids (primarily containing lignin) are used for combined heat and power (CHP) generation using biomass boiler, heat recovery steam generator, and steam turbines (Wan et al. 2016), the needs for natural gas heating and grid electricity can be completely eliminated, such as in case B. Case B with high-yield and on-site CHP generation thus has a reduction in GWP impact by 90%, i.e., 0.7083 kg CO₂ equivalent per kg PHB production, that is, without the consideration of embedded or captured CO₂ in PHB. Figure 14.10 shows the GWP impact proportions of various direct and indirect attributes in case B, without consideration of embedded or captured CO₂ in PHB. The highest to the lowest impact hot spots are sourcing of sodium hydroxide, direct CO₂ emission, and sourcing of SDS, sodium chloride, sulfuric acid, and makeup water, respectively. The GWP was lower than the best value of 1.96 kg CO₂ equivalent per kg PHB production, reported in the literature (Harding et al. 2007). This has been achieved by process integration and optimization strategy developed here.

For the primary impact categories shown in Table 14.6, considerable differences between case B with high-yield and on-site CHP generation and equivalent fossil-based polymer production system exist. The GWP of impact of case B with high-yield and on-site CHP generation here takes account of the embedded or captured

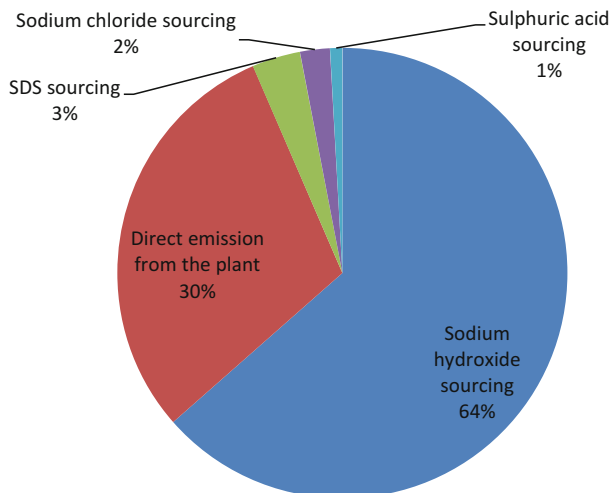


Fig. 14.10 GWP impact proportions of various direct and indirect attributes in case B with high-yield and on-site CHP generation (without the consideration of embedded or captured CO₂ in PHB)

CO₂ in PHB, i.e., = $0.7083 - 2.0465 = -1.3382$ kg CO₂ equivalent per kg PHB production. This gives a percentage reduction in GWP of greater than 100%, while for all other categories, the percentage reduction in environmental impacts is 76–96%. This once again consolidates the importance of process integration tools for integrated biorefinery design. The greater the sourcing of raw materials and energy on-site by in-process material and energy integration, the higher is the sustainability of the integrated biorefinery system.

Performance can still be optimized by reducing the amount of effluents, energy, and chemicals. Biomass pretreatment also plays an important contribution to economic costs, and thus the PHB production may be best when combined with pretreatment technologies other than dilute acid. Furthermore, the separation and conversion of xylose could be beneficial for the overall biorefinery performance.

Take-Home Message

- A set of modeling and analysis tools can be systematically applied for biorefinery development based on extremophile processing, as illustrated for PHB production using halophilic bacteria.
- It is important to relate models at the various scales and to look at the whole process picture to optimize the economic and environmental performances of biorefineries.
- The potential for using halophile bacteria against other technologies is demonstrated to be competitive in terms of economics and environmental impacts; however, high yields and content are required.
- Extremophile processing will play a key role in making biorefineries more profitable and sustainable.

Table 14.6 Primary impacts, for which considerable differences between case B with high-yield and on-site CHP generation and equivalent fossil-based polymer production system exist

Per kg polymer production	Case B: PHB production with CHP generation	Fossil-based equivalent polymer production	Savings by biopolymer production system	% savings by biopolymer
Acidification potential, kg SO ₂ equivalent	0.0032	0.0191	0.0159	83.4846
Eutrophication potential, kg phosphate equivalent	0.0016	0.0137	0.0121	88.2027
Freshwater ecotoxicity potential, kg DCB equivalent	0.2814	1.1807	0.8993	76.1698
GWP, kg CO ₂ equivalent	-1.3382	7.5146	8.8528	117.8074
Human toxicity potential, kg DCB equivalent	0.3856	7.3761	6.9906	94.7726
Marine ecotoxicity potential, kg DCB equivalent	833.6787	3489.2043	2655.5256	76.1069
Urban smog, kg ethylene equivalent	0.0002	0.0042	0.0040	95.5579
Terrestrial ecotoxicity potential, kg DCB equivalent	0.0121	0.0534	0.0413	77.3540
DCB: 1,4-dichlorobenzene				

Acknowledgements Financial support provided by the National Science Foundation in the form of BuG ReMeDEE initiative (Award # 1736255) is gratefully acknowledged by the editors.

References

- Aburto J, Martínez T, Murrieta F (2008) Evaluación técnica-económica de la producción de bioetanol a partir de residuos lignocelulósicos. *Tecnología, Ciencia y Educación* 23(1):23–30
- Barrera I, Amezcua-Allieri MA, Estupiñan L, Martínez T, Aburto J (2016) Technical and economical evaluation of bioethanol production from lignocellulosic residues in Mexico: case of sugarcane and blue agave bagasses. *Chem Eng Res Des* 107:91–101
- Bhalla A, Bansal N, Kumar S, Bischoff KM, Sani RK (2013) Improved lignocellulose conversion to biofuels with thermophilic bacteria and thermostable enzymes. *Bioresour Technol* 128:751–759
- Bosma EF, van der Oost J, de Vos WM, van Kranenburg R (2013) Sustainable production of bio-based chemicals by extremophiles. *Curr Biotechnol* 2:360–379
- Choi J, Lee SY (1997) Process analysis and economic evaluation for poly(3-hydroxybutyrate) production by fermentation. *Bioprocess Eng* 17(6):335–342

- Diario oficial. Ley de promoción y desarrollo de los bionergéticos. Camara de Diputados México (2008) Available from <http://www.diputados.gob.mx/LeyesBiblio/pdf/LPDB.pdf> [21 Feb 2016]
- Dotsch A, Severin J, Alt W, Galinski EA, Kreft JU (2008) A mathematical model for growth and osmoregulation in halophilic bacteria. *Microbiology* 154:2956–2969
- Dumbrepatil A, Adsul M, Chaudhari S, Khire J, Gokhale D (2008) Utilization of molasses sugar for lactic acid production by *Lactobacillus delbrueckii* subsp. *delbrueckii* mutant Uc-3 in batch fermentation. *Appl Environ Microbiol* 74:333–335
- García-Lillo J, Rodríguez-Valera F (1990) Effects of culture conditions on poly(3-hydroxybutyric acid) production by *Haloferax mediterranei*. *Appl Environ Microbiol* 56(8):2517–2521
- Georgieva TI, Mikkelsen MJ, Ahring BK (2007) High ethanol tolerance of the thermophilic anaerobic ethanol producer *Thermoanaerobacter* BG1L1. *Cent Eur J Biol* 2(3):364–377
- González-García Y, Meza-Contreras JC, González-Reynoso O, Córdova-López JA (2013) Síntesis y degradación de polihidroxialcanoatos plásticos de origen microbiano. *Rev Int Contam Ambient* 29:77–115
- Harding KG, Dennis JS, Von Blotnitz H, Harrison STL (2007) Environmental analysis of plastic production processes: comparing petroleum-based polypropylene and polyethylene with biologically-based poly- β -hydroxybutyric acid using life cycle analysis. *J Biotechnol* 130(1):57–66
- ISO 14040. Environmental management – life cycle assessment – principles and framework. ISO 1997. Geneva, Switzerland
- Jin YX, Shi LH, Kawata Y (2013) Metabolomics-based component profiling of *Halomonas* sp. KM-1 during different growth phases in poly(3-hydroxybutyrate) production. *Bioresour Technol* 140:73–79
- King D (2010) The future of industrial biorefineries. World Economic Forum, Switzerland
- Koller M, Muhr A (2014) Continuous production mode as a viable process-engineering tool for efficient poly(hydroxyalkanoate) (PHA) bio-production. *Chem Biochem Eng* 28(1):65–77
- Koller M, Horvat P, Hesse P, Bona R, Kutschera C, Atlic A, Braunegg G (2006) Assessment of formal and low structured kinetic modeling of polyhydroxyalkanoate synthesis from complex substrates. *Bioprocess Biosyst Eng* 29:367–377
- Koller M, Atlic A, Gonzalez-Garcia Y, Kutschera C, Braunegg G (2008) Polyhydroxyalkanoate (PHA) biosynthesis from whey lactose. *Macromol Symp* 272:87–92
- Kumar R, Nanavati H, Noronha SB, Mahajani SM (2006) A continuous process for the recovery of lactic acid by reactive distillation. *J Chem Technol Biotechnol* 81:1767–1777
- Lorantfy B, Seyer B, Herwig C (2014) Stoichiometric and kinetic analysis of extreme halophilic Archaea on various substrates in a corrosion resistant bioreactor. *New Biotechnol* 31(1):80–89
- Martínez-Hernández E, Campbell G, Sadhukhan J (2013a) Economic value and environmental impact (EVEI) analysis of biorefinery systems. *Chem Eng Res Des* 91(8):1418–1426
- Martínez-Hernández E, Sadhukhan J, Campbell GM (2013b) Integration of bioethanol as an in-process material in biorefineries using mass pinch analysis. *Appl Energy* 104:517–526
- Mudliar SN, Vaidya AN, Kumar MS, Dahikar S, Chakrabarti T (2008) Techno-economic evaluation of PHB production from activated sludge. *Clean Techn Environ Policy* 10:255–262
- NNFCC. National Non-Food Crops Centre 2016. www.nnfcc.co.uk [Last accessed Jan 2017]
- Patel M, Ou MS, Ingram LO, Shanmuga KT (2004) Fermentation of sugar cane bagasse hemicellulose hydrolysate to l(+)-lactic acid by a thermotolerant acidophilic *Bacillus* sp. *Biotechnol Lett* 26(11):865–868
- Patel MA, Ou MS, Ingram LO, Shanmugam KT (2005) Simultaneous saccharification and co-fermentation of crystalline cellulose and sugar cane bagasse hemicellulose hydrolysate to lactate by a thermotolerant acidophilic *Bacillus* sp. *Biotechnol Prog* 21:1453–1460
- Ramírez N, Serrano JA, Sandoval H (2006) Microorganismos extremófilos. *Actinomicetos halófilos en México*. *Revista Mexicana de Ciencias Farmacéuticas* 37:56–71
- Rathi DN, Amir HG, Abed RM, Kosugi A, Arai T, Sulaiman O, Hashim R, Sudesh K (2013) Polyhydroxyalkanoate biosynthesis and simplified polymer recovery by a novel moderately halophilic bacterium isolated from hypersaline microbial mats. *J Appl Microbiol* 114(2):384–395

- Sadhukhan J, Ng KS, Martinez-Hernandez E (2014) *Biorefineries and chemical processes: design, integration and sustainability analysis*. Wiley, Chichester
- Satchatippavarn S, Martinez-Hernandez E, Leung Pah Hang MY, Leach M, Yang A (2016) Urban biorefinery for waste processing. *J Chem Eng Res Des* 107:81–90
- Stephanopoulos GN, Aristidou AA, Nielsen J (1998) *Metabolic engineering: principles and methodologies*. Academic Press, San Diego
- Thinkstep Gabi Software (2016) <http://www.gabi-software.com/databases/ecoinvent/> [Last accessed Jan 2017]
- Wan YK, Sadhukhan J, Ng DKS (2016) Techno-economic evaluations for feasibility of sago-based biorefinery, Part 2: Integrated bioethanol production and energy systems. *Chem Eng Res Des* 107:102–116
- Xu M, Smith R, Sadhukhan J (2008) Optimization of productivity and thermodynamic performance of metabolic pathways. *Ind Eng Chem Res* 47(15):5669–5679
- Ye L, Hudari MSB, Li Z, Wu JC (2014) Simultaneous detoxification, saccharification and co-fermentation of oil palm empty fruit bunch hydrolysate for l-lactic acid production by *Bacillus coagulans* JI12. *Biochem Eng J* 83:16–21
- Zambare VP, Bhalla A, Muthukumarappan K, Sani RK, Christopher LP (2011) Bioprocessing of agricultural residues to ethanol utilizing a cellulolytic extremophile. *Extremophiles* 15 (5):611–618